

## Selective Trapping and Retrieval of Single Cells Using Microwell Array Devices Combined with Dielectrophoresis

Misaki HATA, Masato SUZUKI, and Tomoyuki YASUKAWA<sup>†</sup>

Graduate School of Science, University of Hyogo, 3-2-1 Kouto, Kamigori, Ako, Hyogo 678-1297, Japan

We proposed selective manipulation techniques for retrieving and retaining target cells arrayed in microwells based on dielectrophoresis (DEP). The upper substrate with microband electrodes was mounted on the lower substrate with microwells based on the same design of microband electrodes by 90 degree relative to the lower substrate. A repulsive force of negative dielectrophoresis (n-DEP) was employed to retrieve the target cells from the microwell array selectively. Furthermore, the target cells were retained in the microwells after other cells were removed by n-DEP. Thus, the system described in this study could make it possible to retrieve and recover single target cells from a microwell array after determining the function of cells trapped in each microwell.

**Keywords** Dielectrophoresis, cell manipulation, cell array, microwell array, selective retrieval

(Received April 13, 2021; Accepted April 21, 2021; Advance Publication Released Online by J-STAGE April 30, 2021)

Microwell arrays are evolving into an innovative technology to perform functional assays of cells in a single-cell manner and as a template to form homogeneous aggregates of cells, such as spheroids and embryoid bodies (EBs), because microwell arrays allow cells to be placed separately in an array with single cells or in an array with a definitive number of cells, which can then be stimulated with chemical compounds in a parallel format using fluidic flow and incubated on site for a long period of time.<sup>1-3</sup> These technological advantages make it possible to perform functional assays of chemical sensory neurons, including olfactory sensory and cells expressing taste receptors,<sup>4,6</sup> in addition to screening immunological cells, such as lymphocytes and hybridomas.<sup>7-11</sup> The morphological influence analysis of EBs at differentiation was also conducted using microwells.<sup>12,13</sup>

Passive sedimentation has commonly been employed in a parallel arrangement of cells in microwells. The capture efficiency depends on the type of cells, the geometry of the wells (shape, size, and depth), and the properties of the materials forming the wells, which can reach approximately 80% in a single-cell format.<sup>14,15</sup> Alternatively, to increase the number of cells captured in the wells and to achieve a quick formation of the cell arrays, active formats for trapping cells have been demonstrated utilizing micro-fluidic devices,<sup>16,17</sup> acoustic tweezers,<sup>18,19</sup> optoelectronic tweezers,<sup>20</sup> and DEP techniques.<sup>21-24</sup> DEP has become attractive due to its simple, rapid, and massive manipulation of cells. DEP trapping of cells in a fluidic device sandwiched between two conductive substrates has been reported for forming cell arrays with a high density.<sup>25-29</sup> We have previously demonstrated the trapping of cells in microwells at the single-cell level within a few seconds with an occupation efficiency of 95% using a microwell array device.<sup>29-31</sup> However, it has not been possible to regulate the selective manipulation to retrieve certain target cells from the cell array and retain single cells in microwells by removing other cells because the electric

fields generated in each microwell cannot be individually controlled. Currently, the recovery of the target cells after determining the cellular function of individual cells trapped in a cell array employs suction of the target cell in the microwell by a microdispenser. It is necessary to arrange a micropipette above microwells with the target cells by a mechanical micromanipulator, and carefully regulate the collection of each cell. Unfortunately, this method is very time consuming and labor intensive.

This study proposes a simple device for the flexible dielectrophoretic manipulation of cells based on the combination of positive DEP (p-DEP) and negative DEP (n-DEP). The use of the present process allows for retrieval of the target cells from a microwell array, while retaining the target cells by removing undesired cells from the array. Because each microband electrode in the device works independently, a unique procedure was developed for retrieving only the target cell(s) from the arrays. The applied frequency switches from the p-DEP to the n-DEP range on a single pair of microband electrodes above and below the microwell with the target cell(s), and as with other microband electrodes, the applied frequency is maintained in the p-DEP frequency range.

A schematic of the microwell array device is shown in Fig. 1(A). The device comprises indium-tin-oxide (ITO) microband electrodes and ITO microband electrodes with microwell arrays. The microband electrodes were fabricated *via* conventional photolithography and ITO etching processes.<sup>32</sup> Figure 1(B) shows a microscopic image of an ITO microband array with 12-band electrodes (bands 1 – 12) used as an upper substrate in the device. In the image, 9-band electrodes (bands 4 – 12) are shown. The width, gap, and length of the band electrodes were set at 40  $\mu\text{m}$ , 12  $\mu\text{m}$ , and 1.27 mm, respectively. We also prepared ITO microband array electrodes with the same design (band A-I) to fabricate microwell arrays. Figure 1(C) shows an image of microwell arrays (16  $\mu\text{m}$  in diameter, 10  $\mu\text{m}$  in depth, and a 12  $\times$  12 well configuration) fabricated on microband array electrodes using negative photoresist SU-8 3010 (MicroChem Corp., Westborough, MA, USA), which was

<sup>†</sup> To whom correspondence should be addressed.  
E-mail: yasu@sci.u-hyogo.ac.jp

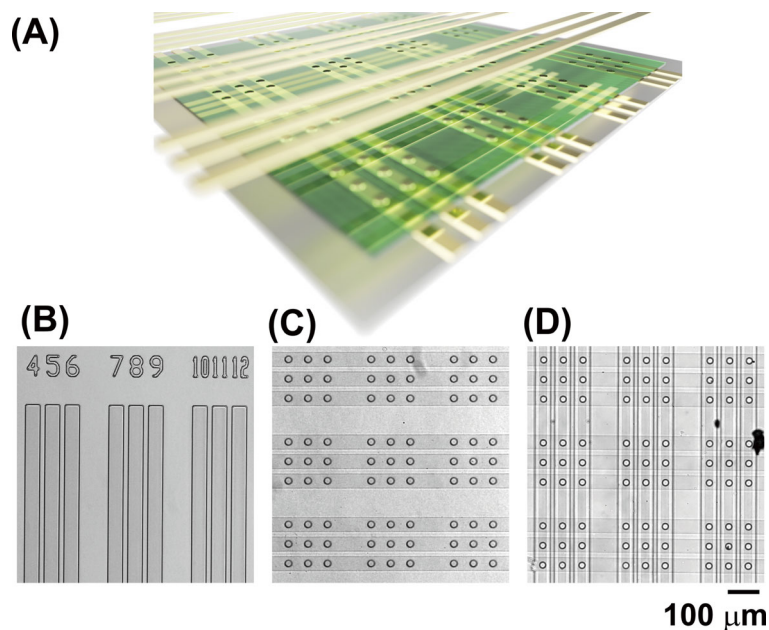


Fig. 1 (A) Schematic of the microwell array device comprising the upper microband electrodes and the lower microband electrodes with the microwell array. (B) Optical image of microband array electrodes used as the upper substrate. (C) Optical image of microband array electrodes with microwell array used as the lower substrate. (D) Optical image of microwell array device that was fabricated by mounting the upper band electrodes (Fig. 1(B)) on the lower band electrodes with the microwell array (Fig. 1(C)).

used as the lower substrate. The center distance between neighboring wells was set at  $52\ \mu\text{m}$ . For assembling the microwell array devices, the substrate with the microband array electrode was mounted on the substrate with the microwell array fabricated on microband electrodes with an orthogonal arrangement by employing a double-sided adhesion sheet ( $30\ \mu\text{m}$  in thickness, Nitto Denko Corp., Osaka Japan) with an I shape ( $8\ \text{mm}$  in width and  $28\ \text{mm}$  in length) to include a microfluidic channel (Fig. S1). Microband array electrodes on the upper substrate were located immediately above the microwells on the lower substrate to form 144 intersections comprising microband electrodes containing microwells (Fig. 1(D)). Two holes ( $0.6\ \text{mm}$  in diameter) were etched on the upper substrate at  $20\ \text{mm}$  intervals using a  $\text{CO}_2$  laser (VLS2.30, UNIVERSAL Laser Systems, Inc., Scottsdale, AZ, USA) for its use as inlets and outlets of the microfluidic channels.

A mouse myeloma cell line PAI (kindly supplied by Prof. Tomita at Mie University) was maintained in an RPMI 1640 medium supplemented with 10% (v/v) fetal bovine serum (Thermo Fisher Scientific, Inc.), 50 units/mL of penicillin, and  $50\ \mu\text{g/mL}$  of streptomycin at  $37^\circ\text{C}$  in a 5%  $\text{CO}_2$  incubator. To perform fluorescence imaging, myeloma cells were stained with Calcein-AM (Dojindo Laboratories Inc., Kumamoto, Japan) and/or CytoRed (Dojindo Laboratories Inc.) following a manual supplied by the company. These dyes were added to the cell suspension at final concentrations of 1 and  $5\ \mu\text{M}$ , respectively.

For dielectrophoretic manipulation of cells by the microwell array device with 3-D microband electrodes, cells were resuspended in the DEP medium comprising 200 mM sucrose, 40 mM NaOH, and 16 mM HEPES (pH 7.7, conductivity  $90\ \text{mS/m}$ ). The fluidic channel of the device was treated with  $\text{O}_2$  plasma for 5 min, and then filled with an aqueous solution containing  $10\ \text{mg/mL}$  bovine serum albumin for an hour to prevent any non-specific adsorption of cells. After introducing  $10\ \mu\text{L}$  of the cell suspension ( $\sim 3.0 \times 10^7$  cells/mL) in the

channel, a sinusoidal signal (1 – 5 Vpp, 150 kHz – 3 MHz) was applied to the microband electrodes using a function generator (7075 waveform generator, HIOKI E. E. Corp., Nagano, Japan).

To prepare a cell array, a half-and-half mixture suspension ( $3.0 \times 10^7$  cells/mL) of myeloma cells, stained in green by Calcein-AM and stained in red by CytoRed, was introduced in the channel at a flow rate of  $30\ \mu\text{L/min}$ . Figure 2(A) shows a top view of the device. An AC signal (1 MHz, 5 Vpp) was applied to the upper 12 microband electrodes, while an AC signal with the same voltage and frequency and the opposite phase was applied to the lower 12 microband electrodes. Figure 2(B) presents a fluorescent image showing the formation of the cell array with myeloma cells stained in green or red. The cells that flowed randomly in the channels began to move until they were trapped in the microwells by the p-DEP immediately after the AC signal was applied, which resulted in the formation of the cell array within a few seconds. Then, the DEP medium without cells was introduced in the channel to remove any excess cells. The observation of green or red signals in each microwell denotes that individual cells were trapped in each microwell. Figure 2(C) shows a cross-sectional view of the device along with microband electrode 2 in the upper substrate, as can be seen in Fig. 2(A). This illustration suggests that the strong electric fields formed in the microwells owing to the restricted conductive region of the bottom substrate created by the negative photoresist were used to form the microwell array. The cell occupation efficiencies in the microwells with single cells were 42 and 46% for green and red cells, respectively. Thus, the efficiency could be estimated, and was found to be approximately 90%. This result indicated that the cell array could be rapidly and efficiently formed by p-DEP manipulation.

We also demonstrated the retrieval of a single target cell from a cell array formed by n-DEP. Mixtures ( $3.0 \times 10^6$  cells/mL) of cells stained in green and red were prepared in a ratio of 10:1 to demonstrate the retrieval of red cell(s) designated as the target

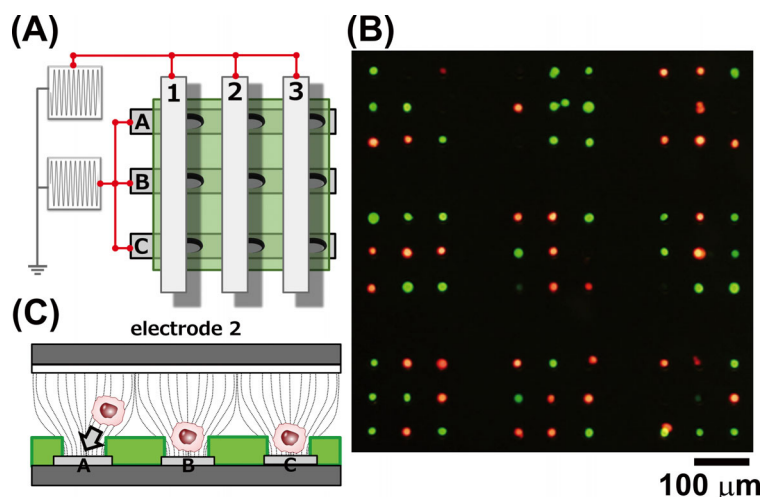


Fig. 2 (A) Top view of the microwell array device. (B) Fluorescence image of myeloma cells stained in green or red captured in the microwell. (C) Cross-sectional view of the device along electrode 2 in Fig. 2(A). Dotted lines show the pseudo lines of the electric forces.

cell. Again, the application of the AC signal (1 MHz, 3 Vpp) to both the upper and the lower microband electrodes with opposite phasing resulted in the formation of the cell array. A single red cell was trapped in the 3-I well and eight green cells were trapped in the others (Fig. 3(A-1)). White dotted lines in Fig. 3 show the edges of both upper and lower band electrodes. Subsequently, the frequency applied to band electrode 3 on the upper substrate and the band electrode I on the lower substrate was switched from 1 MHz for p-DEP to 300 kHz for n-DEP, while the frequency applied to the other band electrodes was maintained at 1 MHz for p-DEP (Fig. 3(A-2)). Figure 3(A-3) shows fluorescent image of the cell pattern in the microwell arrays after switching the frequency for band electrodes 3 and I. The target red cell in the 3-I well was gradually removed over a few seconds after switching the frequency, and it was then transferred downward in the image by slight fluidic flow. In contrast, the other green cells remained in the original position. The results indicated that the repulsive force of n-DEP from the strong electric field region acts on the cell in the 3-I well that comprises both band electrodes switched in the n-DEP frequency region. It is noted that p-DEP still acted on cells in wells comprising band electrodes that applied an AC signal in the p-DEP and n-DEP frequency regions, respectively (*e.g.*, wells 2-I and 3-G). Thus, this system would make it possible to retrieve target cells selectively from the array of cells and recover them in an outlet without the microdispensers after removing the upper substrate.

However, cells in microwells adjacent to the microwell with the target cell were also removed when the voltage for band electrodes, except for the band electrode with the microwells containing the target cells, was switched off (Fig. S2). After the cell-based array was formed by p-DEP, the frequency applied to band electrodes 2 and H was switched to the n-DEP region, and the signal for the other band electrodes was switched off (Fig. S2(A)). The cell trapped in the 2-H well was gradually removed from the well by n-DEP approximately 5 s after the frequency was switched. However, the cells trapped in wells 1-H and 3-H were also removed from their wells 60 s after switching (Fig. S2(B)). This removal of undesired cells trapped in microwells was responsible for generating a weak electric field in wells 1-H and 3-H due to applying an AC signal to band electrode 2 and H in the opposite phase. Therefore, the

application of a p-DEP AC signal to the band electrodes, except for the electrodes with the microwells containing the target cells, was absolutely required to accurately retrieve the target cells.

Finally, we demonstrated that the target cell trapped in the well was maintained in the well by p-DEP, while the other cells were removed from each well by n-DEP (Fig. 3(B)). In this experiment, a mixture of cells stained in green and cells stained in both green and red was injected into the channel at a ratio of 10:1. After forming the cell-based array by applying an AC signal, two double-staining cells (yellow) were trapped in wells 4-H and 5-I (Fig. 3(B-1)). The AC signal (2 Vpp, 1 MHz) applied to band electrodes, except for band electrodes 5 and I was switched to the signal with 3 Vpp and 150 kHz (Fig. 3(B-2)). Figure 3(B-3) shows the image of the double-staining cells trapped in well 5-I. The cells trapped in wells, except well 5-I, were removed from each well after switching the AC signal, and further moved downstream by fluidic flow (30  $\mu$ L/min). The cells in well 5-I experienced the p-DEP force due to the application of p-DEP (1 MHz), while the cells in wells 4-G, 4-H, 6-G, and 6-H wells experienced the n-DEP force upon applying n-DEP (150 kHz) from both the upper and lower electrodes. However, the cells in wells 4-I, 6-I, 5-G, and 5-H exposed to the electric field when both frequencies p-DEP (1 MHz) and n-DEP (150 kHz) were mixed and applied. The application of the relatively high n-DEP (3 Vpp) compared to that for p-DEP (2 Vpp) gave rise to the repulsive force of n-DEP for those cells. Unfortunately, the cell in well 6-G remained in the well. This may have been due to the non-specific adsorption of cells to the wall and the bottom of the well. Thus, the use of the present device makes it possible to retrieve single target cells from a cell-based array, and to retain single target cells after removing cells in the other wells.

In conclusion, the highly-flexible and highly-precise handling of cells in a single-cell manner was achieved by using the novel microwell array device incorporating a 3-D microband array with an orthogonal arrangement. We developed the techniques to retrieve single target cells from a cell array and to retain single target cells in the microwell array by regulating the frequency and voltage applied to the upper and the lower microband electrodes. We will apply the present technologies to discriminate and recover cells with specific functions, such as cells expressing specific surface antigens, cells secreting specific

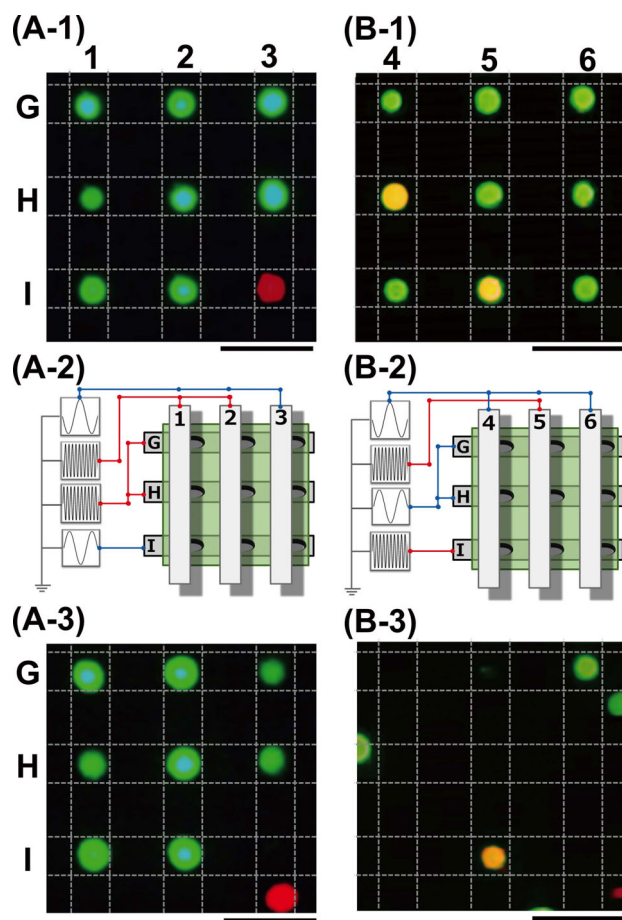


Fig. 3 (A-1) Fluorescence image of the array of cells stained in green or red. (A-2) Top view of the microwell array device for describing the application of AC signals to retrieve a target cell in microwell 3-I. (A-3) Fluorescence image showing retrieval of the target cell in microwell 3-I from the cell array. (B-1) Fluorescence image of the array of cells stained in green and cells stained in both green and red (yellow). (B-2) Top view of the microwell array device for describing the application of AC signals to retain a target cell in the microwell 5-I. (B-3) Fluorescence image showing retention of the target cell in the microwell 5-I. The bar scale was 100  $\mu\text{m}$ .

antibodies, and cells secreting cytokines (such as interleukin, chemokine, interferon, and growth factors). The novel microwell array device can contribute to the functional screening of special cells and the functional analysis of rare cells, such as circular tumor cells and induced pluripotent stem cells from cell populations.

### Acknowledgements

This work was partly supported by JSPS KAKENHI Grant Number 19K05548 and 20H02771.

### Supporting Information

Supporting Information includes Fig. S1 for the whole design of the device fabricated and Fig. S2 for retrieving of a target cell. This material is available free of charge on the Web at <http://www.jsac.or.jp/analsci/>.

### References

1. T. Konry, S. Sarkar, P. Sabhachandani, and N. Cohen, *Annu.*

*Rev. Biomed. Eng.*, **2016**, *18*, 259.

2. L. Armbrrecht and P. S. Dittrich, *Anal. Chem.*, **2017**, *89*, 2.
3. H. Park, H. Kim, and J. Doh, *Bioconjug. Chem.*, **2018**, *29*, 672.
4. X. A. Figueroa, G. A. Cooksey, S. V. Votaw, L. F. Horowitz, and A. Folch, *Lab Chip*, **2010**, *10*, 1120.
5. M. Suzuki, N. Yoshimoto, K. Shimono, and S. Kuroda, *Sci. Rep.*, **2016**, *6*, 19934.
6. Y.-H. Hsiao, C.-H. Hsu, C. Chen, Y.-H. Hsiao, C.-H. Hsu, and C. Chen, *Molecules*, **2016**, *21*, 896.
7. S. Yamamura, H. Kishi, Y. Tokimitsu, S. Kondo, R. Honda, S. Ramachandra Rao, M. Omori, E. Tamiya, and A. Muraguchi, *Anal. Chem.*, **2005**, *77*, 8050.
8. A. O. Ogunniyi, C. M. Story, E. Papa, E. Guillen, and J. C. Love, *Nat. Protoc.*, **2009**, *4*, 767.
9. A. Jin, T. Ozawa, K. Tajiri, T. Obata, H. Kishi, and A. Muraguchi, *Nat. Protoc.*, **2011**, *6*, 668.
10. J. C. Love, J. L. Ronan, G. M. Grotenbreg, A. G. van der Veen, and H. L. Ploegh, *Nat. Biotechnol.*, **2006**, *24*, 703.
11. Q. Han, N. Bagheri, E. M. Bradshaw, D. A. Hafler, D. A. Lauffenburger, and J. C. Love, *Proc. Natl. Acad. Sci.*, **2012**, *109*, 1607.
12. Y.-S. Hwang, B. G. Chung, D. Ortmann, N. Hattori, H.-C. Moeller, and A. Khademhosseini, *Proc. Natl. Acad. Sci. U. S. A.*, **2009**, *106*, 16978.
13. G. Pettinato, X. Wen, and N. Zhang, *Sci. Rep.*, **2015**, *4*, 7402.
14. J. R. Rettig and A. Folch, *Anal. Chem.*, **2005**, *77*, 5628.
15. L. Huang, Y. Chen, Y. Chen, and H. Wu, *Anal. Chem.*, **2015**, *87*, 12169.
16. A. M. Skelley, O. Kirak, H. Suh, R. Jaenisch, and J. Voldman, *Nat. Methods*, **2009**, *6*, 147.
17. J. F. Swennenhuis, A. G. J. Tibbe, M. Stevens, M. R. Katika, J. van Dalum, H. Duy Tong, C. J. M. van Rijn, and L. W. M. M. Terstappen, *Lab Chip*, **2015**, *15*, 3039.
18. J. Shi, D. Ahmed, X. Mao, S.-C. S. Lin, A. Lawit, and T. J. Huang, *Lab Chip*, **2009**, *9*, 2890.
19. D. J. Collins, B. Morahan, J. Garcia-Bustos, C. Doerig, M. Plebanski, and A. Neild, *Nat. Commun.*, **2015**, *6*, 8686.
20. Y. Yang, Y. Mao, K.-S. Shin, C. O. Chui, and P.-Y. Chiou, *Sci. Rep.*, **2016**, *6*, 22630.
21. M. Şen, K. Ino, J. Ramón-Azcón, H. Shiku, and T. Matsue, *Lab Chip*, **2013**, *13*, 3650.
22. S. H. Kim and T. Fujii, *Lab Chip*, **2016**, *16*, 2440.
23. C. Wu, R. Chen, Y. Liu, Z. Yu, Y. Jiang, and X. Cheng, *Lab Chip*, **2017**, *17*, 4008.
24. Y. Wu, Y. Ren, Y. Tao, L. Hou, and H. Jiang, *Anal. Chem.*, **2018**, *90*, 11461.
25. T. Murata, T. Yasukawa, H. Shiku, and T. Matsue, *Biosens. Bioelectron.*, **2009**, *25*, 913.
26. A. Morimoto, T. Mogami, M. Watanabe, K. Iijima, Y. Akiyama, K. Katayama, T. Futami, N. Yamamoto, T. Sawada, F. Koizumi, and Y. Koh, *PLoS One*, **2015**, *10*, e0130418.
27. H. Okayama, M. Tomita, M. Suzuki, and T. Yasukawa, *Anal. Sci.*, **2019**, *35*, 701.
28. T. Yasukawa, A. Morishima, M. Suzuki, J. Yoshioka, K. Yoshimoto, and F. Mizutani, *Anal. Sci.*, **2019**, *35*, 895.
29. Y. Yoshimura, M. Tomita, F. Mizutani, and T. Yasukawa, *Anal. Chem.*, **2014**, *86*, 6818.
30. Y. Yoshimura, C. Fujii, M. Tomita, F. Mizutani, and T. Yasukawa, *Chem. Lett.*, **2014**, *43*, 980.
31. R. Takeuchi, M. Suzuki, and T. Yasukawa, *Anal. Sci.*, **2021**, *37*, 229.
32. H. Hatanaka, T. Yasukawa, and F. Mizutani, *Anal. Chem.*, **2011**, *83*, 7207.